A SHORT REVIEW OF BLOOD FLOW MODELLING METHODS: FROM MACRO- TO MICROSCALES

KATARZYNA KACZOROWSKA AND KRZYSZTOF TESCH

Gdansk University of Technology
G. Narutowicza 11/12, 80-233 Gdansk, Poland

(received: 15 November 2016; revised: 9 December 2016;
accepted: 15 December 2016; published online: 2 January 2017)

Abstract: The aim of this paper it to review various scale approaches to the blood flow modelling. Blood motion may be described by three types of mathematical models according to the observed scales or resolutions, namely microscopic, mesoscopic and macroscopic descriptions. The above approaches are discussed together with their advantages and disadvantages. Several results of mesoscopic simulations are presented with particular attention paid to mesoscale semi-continuum models suitable for real-time blood flow visualisation.

Keywords: blood flow, red blood cells, mesoscale models
DOI: https://doi.org/10.17466/tq2017/21.1/a

Notation

A	area
$\boldsymbol{A}_i$	Rivlin-Ericksen tensor
$\boldsymbol{C}_t$	left Cauchy-Green tensor
$\boldsymbol{D}$	strain rate tensor
E	energy
f	function, probability distribution function
$\boldsymbol{f}$, $\boldsymbol{F}$	force
$\boldsymbol{g}$, $\boldsymbol{G}$	gravitational acceleration
k	constant, spring constant
L	length
m	mass
$\boldsymbol{r}$	distance, position
$\hat{\boldsymbol{n}}$	normal unit vector
N	number of particles
p	pressure
S	surface area
t	time
$\boldsymbol{u}$	velocity vector

$\boldsymbol{v}$ particle velocity
V potential, volume
$\hat{\boldsymbol{w}}$ unit vector
x_i coordinates

β damping constant
γ shear rate, bending constant
$\boldsymbol{\delta}$ Kronecker delta
ε depth of the potential well
θ angle
κ non-linearity function
λ_1 relaxation time
λ_2 retardation time
μ dynamic viscosity
ρ density
σ finite distance
$\boldsymbol{\sigma}$ stress tensor
τ time
$\boldsymbol{\tau}$ viscous part of the stress tensor
Ω collision operator

$|\cdot|$ cardinality of a set
∇ gradient
$\nabla\cdot$ divergence
$\frac{\mathrm{d}}{\mathrm{dt}}$ substantial derivative

1. Introduction

Blood is a suspension of blood cells in the plasma. The presence of red blood cells is responsible for the non-Newtonian blood nature. A proper approach allowing complete or nearly complete modelling of the blood flow behaviour should take into consideration the presence, flexibility and aggregation of red blood cells. Furthermore, the influence of temperature on the viscosity, the membrane thermal fluctuations and the yield stress are also important.

Blood motion may be described by three types of mathematical models according to the observed scales. The typical methods associated with specific scales are the following:

- Macroscopic description (continuum)
  - Classical fluid mechanics
- Mesoscopic description
  - Lattice Boltzmann method
  - Dissipative particle dynamics
  - Brownian dynamics
  - Smoothed particle hydrodynamics
- Microscopic description
  - Molecular dynamics
  - Monte Carlo method

Typically, the macroscale approach cannot satisfy all the attributes of blood. However, this method is useful in order to simulate the blood flow for large space (arteries), see Figure 1. A continuum method is suitable for vessels larger than 100 μm. One has to keep in mind that non-Newtonian constitutive equations are required in the range 0.1 to 1 mm.

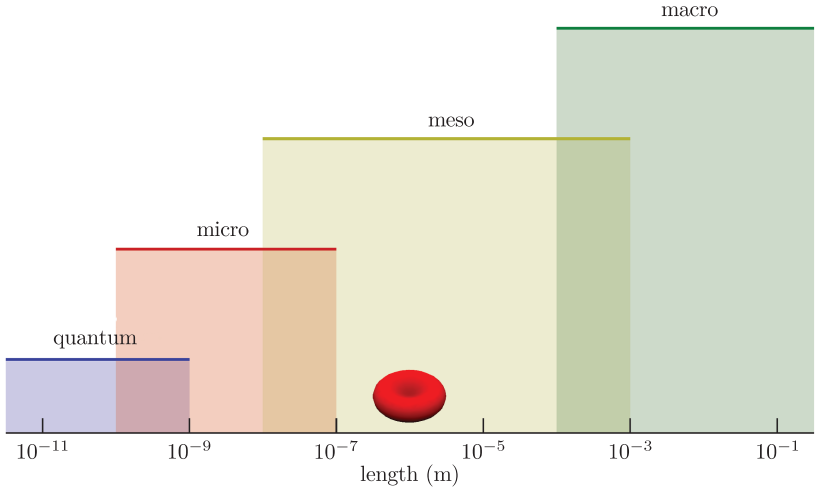

Figure 1. Length scales

When it comes to capillaries, *i.e.* diameters are smaller than 100 μm, explicit modelling of red blood cells is required. This is because the prediction of continuum models breaks down entirely. An average diameter of red blood cells is about 8 μm. This means that at least mesoscopic modelling is necessary, see Figure 1, involving lattice Boltzmann [1, 2], dissipative [3] and smoothed particle dynamics [4] methods.

Methods involving modelling of the motion of red blood cells can be divided into rigid and flexible. The latter, being the most interesting and advanced, can be further classified into spring-damper like models [5], the spectrin network model [6, 7] and the elastic immersed boundary model [5]. Generally speaking, various methods of blood flow modelling can be classified as follows:

- Single-phase flow
  - Newtonian fluid
  - Non-Newtonian fluids
- Two-phase flow
  - Passive transport
    - Rigid RBC
    - Flexible RBC
  - Active transport (fluid-structure interaction)
    - Rigid RBC
    - Flexible RBC

Another classification of methods of blood flow modelling with deformable red blood cells can be divided into:

- fully continuum, *i.e.* continuum fluid and RBC solid,
- semi-continuum, *i.e.* continuum fluid and discrete RBC solid,
- particle, *i.e.* discrete fluid and RBC solid.

For instance, Figure 2 presents example simulation results of passive transport of rigid red blood cells in the Hagen-Poiseuille flow. This can also be classified as a semi-continuum approach with a continuum fluid and discrete red blood cells.

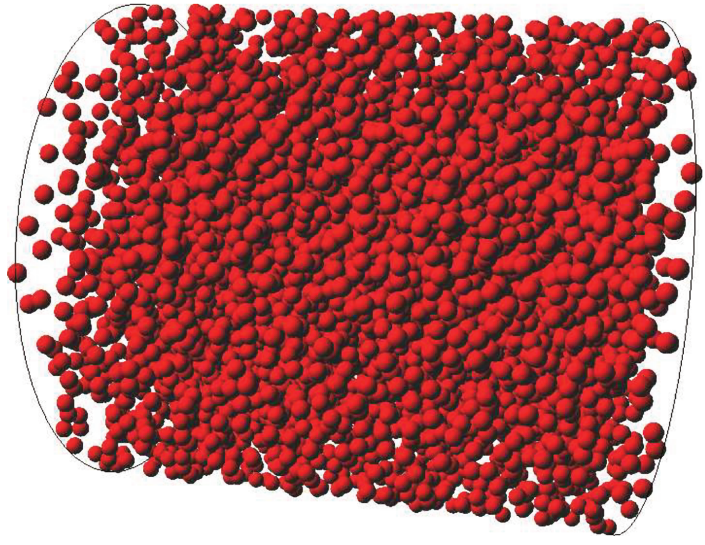

Figure 2. Passive transport of rigid RBCs

2. Macroscale approach

Although blood is a suspension of blood cells in the plasma [8], the blood flow in large vessels is regarded as a single-component and single-phase fluid. The non-Newtonian phenomena, such as shear thinning, yield stress and constant viscosity values at high shear rates are modelled by means of a proper constitutive equation.

The closed system of equations for laminar, incompressible, both Newtonian and non-Newtonian fluids consists of the continuity equation

$$\nabla \cdot \boldsymbol{u} = 0 \tag{1}$$

and the linear momentum conservation equation

$$\rho \frac{\mathrm{d}\boldsymbol{u}}{\mathrm{dt}} = \rho \boldsymbol{g} + \nabla \cdot \boldsymbol{\sigma} \tag{2}$$

In the above, $\boldsymbol{u}$ denotes the velocity vector, $\boldsymbol{g}$ stands for the gravitational acceleration (the mass force only is considered here), p indicates pressure, ρ density

and the viscous part of the stress tensor is denoted as $\boldsymbol{\tau}$. Typically, $\boldsymbol{\sigma} = -p\boldsymbol{\delta} + \boldsymbol{\tau}$. This provides the second form of the conservation of linear momentum

$$\rho \frac{\mathrm{d}\boldsymbol{u}}{\mathrm{dt}} = \rho \boldsymbol{g} - \nabla p + \nabla \cdot \boldsymbol{\tau} \tag{3}$$

Another, so-called rheological constitutive equation is needed in order to close the above system. We can divide rheological constitutive equations into categories of Newtonian-, generalised Newtonian-, differential-, integral- and rate type fluids [9]. The Newtonian hypothesis is given by

$$\boldsymbol{\tau} = 2\mu \boldsymbol{D} \tag{4}$$

Generalised Newtonian fluids satisfy the following rheological equation

$$\boldsymbol{\tau} = 2\mu(\gamma)\boldsymbol{D} \tag{5}$$

The second invariant of the strain rate tensor $\boldsymbol{D}$ is given by $\gamma^2 = 2\boldsymbol{D}^2$. For differential type fluids the viscous part of the stress tensor $\boldsymbol{\tau}$ is expressed explicitly as a function of other kinematic tensors and their derivatives

$$\boldsymbol{\tau} = f(\boldsymbol{A}_1, \boldsymbol{A}_2, ...) \tag{6}$$

where

$$\boldsymbol{A}_{i+1} = \frac{\mathrm{d}\boldsymbol{A}_{\mathrm{i}}}{\mathrm{dt}} + \boldsymbol{A}_i \cdot (\nabla \boldsymbol{u})^{\mathrm{T}} + \nabla \boldsymbol{u} \cdot \boldsymbol{A}_i, \quad i = 1, 2, ... \tag{7}$$

For the rate type fluids this equation is not explicit $\dot{\boldsymbol{\tau}} = f(\boldsymbol{\tau}, \boldsymbol{D}, \dot{\boldsymbol{D}})$. The dot represents the frame-invariant derivative. For instance we have

$$\boldsymbol{\tau} + \lambda_1 \dot{\boldsymbol{\tau}} = 2\mu \left(\boldsymbol{D} + \lambda_2 \dot{\boldsymbol{D}} \right) \tag{8}$$

Finally, for the integral type fluids the viscous part of the stress tensor is expressed explicitly as a function of one or more integrals of other kinematic tensors

$$\boldsymbol{\tau} = \int_{-\infty}^{t} f(t-\tau) \left(\boldsymbol{\delta} - \boldsymbol{C}_t(\tau) \right) \mathrm{d}\tau \tag{9}$$

The generalised Newtonian fluids are the simplest and easiest to implement into the existing CFD codes [10]. More advanced models such as differential- and rate type fluids are able to better approximate blood features but they cannot be directly implemented into the existing CFD codes. What is more, even the most advanced constitutive equations cannot satisfy all the attributes of blood. Apart from the non-Newtonian properties of blood, other challenging difficulties [11] are the complex and variable geometry and the flexible and non-linear properties of blood vessels as well as the transient nature of the blood flow.

Furthermore, the macroscale approach based on the momentum conservation equation is not particularly suitable for the real-time visualisation of the blood flow. Although, the macroscopic approach is able to simulate the blood flow for large space and time scales (large arteries) [12, 13], it breaks down entirely in capillaries. This is because non-Newtonian properties of blood are important in

vessels with a diameter smaller than 1 mm. Explicit modelling of red blood cells is required for arteries of diameters smaller than about 100-200 μm.

3. Microscale approach

Molecular dynamics takes advantage of classical mechanics equations in order to model molecular systems in the context of the N-body simulation. The motion of molecules is determined by solving Newton's equation of motion

$$m_i \frac{\mathrm{d}^2 \boldsymbol{r}_\mathrm{i}}{\mathrm{dt}^2} = \boldsymbol{G}_i + \sum_{j=1 \neq i}^{N} \boldsymbol{f}_{ij} \tag{10}$$

The force exerted on a molecule consists of an external force such as gravity $\boldsymbol{G}_i$ and the intermolecular force $\boldsymbol{f}_{ij} = -\nabla V$, generally described by means of the Lennard-Jones potential

$$V = 4\epsilon \left(\left(\frac{\sigma}{r} \right)^{12} - \left(\frac{\sigma}{r} \right)^{6} \right) \tag{11}$$

Molecular dynamics is able to simulate the blood behaviour to the finest detail, however, the length and time scales are limited to small atomistic scales. What is more, the molecular dynamics approach requires an extremely high computational cost. In order to overcome these difficulties, the so-called coarse-grained models are necessary. These are classified as mesoscopic models and are still able to capture certain molecular phenomena.

4. Mesoscale approach

The individual vertex i of the red blood cell membrane surface moves according to

$$m \frac{\mathrm{d}^2 \boldsymbol{r}_\mathrm{i}}{\mathrm{dt}^2} = \boldsymbol{G}_i + \boldsymbol{F}_i \tag{12}$$

The force exerted on a vertex consists of an external force (gravity) $\boldsymbol{G}_i$ and an additional force $\boldsymbol{F}_i$ according to specific models.

4.1. Dissipative particle dynamics

The DPD [14] method simulates a reduced number of degrees of freedom (coarse-grained models) only. All the red blood cells (the membrane and its interior) and the blood plasma are modelled by means of DPD, see Figure 3. The motion of plasma and internal membrane liquid particles is determined by solving Newton's equation of motion

$$m \frac{\mathrm{d}^2 \boldsymbol{r}_\mathrm{i}}{\mathrm{dt}^2} = \sum_{j=1 \neq i}^{N} \left(\boldsymbol{f}_{ij}^C + \boldsymbol{f}_{ij}^D + \boldsymbol{f}_{ij}^R \right) \tag{13}$$

where the interaction forces are the sum of conservative $\boldsymbol{f}_{ij}^C$ or repulsion forces, dissipative forces $\boldsymbol{f}_{ij}^D$ and random force $\boldsymbol{f}_{ij}^R$.

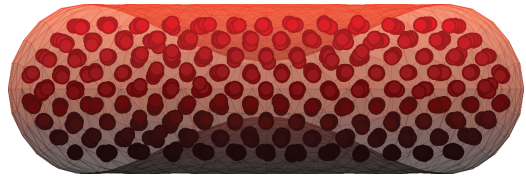

Figure 3. DPD particles inside RBC

For the membrane particles we have equation (12) with $\boldsymbol{F}_i$ [3]

$$\boldsymbol{F}_i = \boldsymbol{f}_i^M + \boldsymbol{f}_i^{PP} + \sum_{j=1\neq i}^{N} \left(\boldsymbol{f}_{ij}^C + \boldsymbol{f}_{ij}^D + \boldsymbol{f}_{ij}^R \right) \tag{14}$$

where $\boldsymbol{f}_i^M$ is the membrane force, which is discussed further below and $\boldsymbol{f}_i^{PP}$ is the inter-cellular force responsible for the cell to cell interaction. The inter-cellular force can be modelled, for instance, by means of the Morse potential [3].

4.2. Lattice Boltzmann method

The lattice Boltzmann [15] method is suitable only for blood plasma flow modelling. The Chapman-Enskog expansion makes it possible to recover the incompressible Navier-Stokes equations for low Reynolds numbers. This is suitable for blood plasma simulation. The continuous Boltzmann equation

$$\frac{\partial f}{\partial t} + \boldsymbol{v} \cdot \nabla f = \Omega(f) \tag{15}$$

with proper collision operator Ω is taken into consideration. The BGK (Bhatnagar-Gross-Krook) approximation $\Omega(f) = \tau^{-1}(f^{eq} - f)$ is the most popular simplification of the collision operator. The velocity space $\boldsymbol{v}$ is then discretised into a finite set of $\{\boldsymbol{v}_n\}$, resulting in the discrete Boltzmann equation. Finally, the lattice Boltzmann equation can be formulated

$$f_n(\boldsymbol{r} + \boldsymbol{v}_n \Delta t, t + \Delta t) - f_n(\boldsymbol{r}, t) = \frac{1}{\hat{\tau}} \left(f_n^0(\boldsymbol{r}, t) - f_n(\boldsymbol{r}, t) \right) \tag{16}$$

where $\hat{\tau}$ is the dimensionless relaxation time. Eventually, after performing collisions and streaming steps over a discrete lattice, it is possible to find the discrete probability distribution function f_n. Macroscopic variables, such as velocity, can be recovered from the distribution function. Furthermore, coupling the red blood cell membranes with a fluid domain resolved by the lattice-Boltzmann method, allows active transport and cells deformation. This can be achieved by means of the spectrin network model or the elastic immersed boundary model, which are discussed further below.

4.3. Spring-damper model

For spring-damper like models (Figure 4) we have equation (12) with

$$\boldsymbol{F}_i = \boldsymbol{f}_{is} + \boldsymbol{f}_{id} + \boldsymbol{f}_{ib} \tag{17}$$

where $\boldsymbol{f}_{is}$ are spring forces, $\boldsymbol{f}_{id}$ – damper forces and $\boldsymbol{f}_{ib}$ – bending forces. Also, local and global conservative forces can be applied if the spring-damper network represents a closed surface.

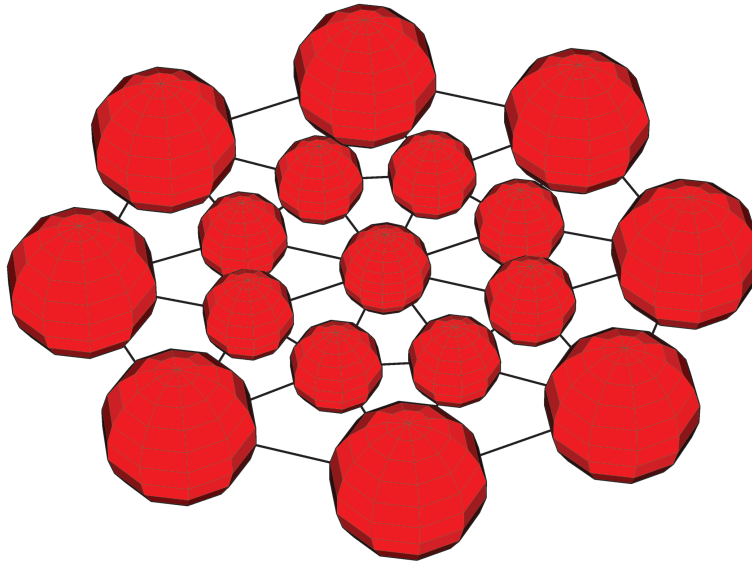

Figure 4. Spring-damper model

The spring forces

$$\boldsymbol{f}_{is} = -k \sum_{j \in N_b} \Delta \boldsymbol{r}_{ij} \tag{18}$$

are proportional to the instantaneous (stretched or compressed) length $r_{ij}(t)$ relative to the spontaneous length $r_{ij}(t_0)$, that is to say

$$\Delta \boldsymbol{r}_{ij} = \big(r_{ij}(t) - r_{ij}(t_0)\big)\, \hat{\boldsymbol{r}}_{ij}(t) \tag{19}$$

The spring constant is denoted as k and $\hat{\boldsymbol{r}}_{ij}(t)$ is the unit vector pointing from the centre of two particles. Finally, N_b stands for all the neighbours of a selected particle. Equation (18) expresses Hooke's law. Springs are always associated with dampers in order to suppress oscillations. The damper forces are proportional to particle velocity $\boldsymbol{v}_i$ and are necessary in order to smooth out the motion between particles

$$\boldsymbol{f}_{id} = -2\beta \boldsymbol{v}_i - 2\beta_* \sum_{j \in N_b} \Delta \hat{\boldsymbol{r}}_{ij} \big(\Delta \boldsymbol{v}_{ij} \cdot \Delta \hat{\boldsymbol{r}}_{ij}\big) \tag{20}$$

The damping constant is is denoted as β. Additional damping constant β_* is useful when one wants to suppress only oscillations, rather than the total motion.

Finally, bending forces are necessary to preserve the spontaneous shape of red blood cells. The simplest equation has the following form

$$\boldsymbol{f}_{ib} = \frac{\gamma}{|N_b|} \sum_{j \in N_b} \big(\boldsymbol{r}_i - \boldsymbol{r}_j\big) \tag{21}$$

where γ is the bending constant. One has to make sure that the total force acting on a particle is zero. In order to satisfy this condition, the opposite forces are necessary for all $|N_b|$ neighbouring particles

$$\boldsymbol{f}_{jb} = \frac{-\boldsymbol{f}_{ib}}{|N_b|} \tag{22}$$

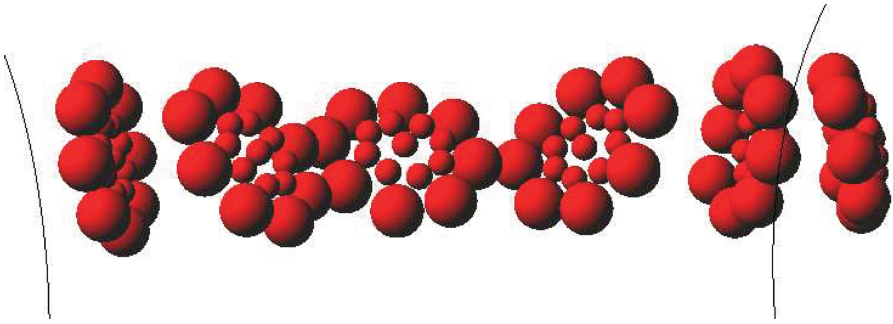

Figure 5. Simulation of a single RBC by means of the spring-damper model

Figure 5 presents example simulation results of a single flexible red blood cell in the Hagen-Poiseuille flow. This again can be classified as a semi-continuum approach with a continuum fluid and discrete red blood cells.

4.4. Spectrin network model

The spectrin network method considers the red blood cell membrane as a network of triangles and vertices (Figure 6). The force exerted on a vertex consists of

$$\boldsymbol{F}_i = \boldsymbol{f}_i^{FS} + \boldsymbol{f}_i^{PP} + \boldsymbol{f}_i^{M} \tag{23}$$

The external forces due to the fluid-structure interaction on a vertex are denoted as $\boldsymbol{f}_i^{FS}$, where $\boldsymbol{f}_i^{PP}$ represents forces due to particle-particle interaction. The forces due to the Helmholtz free energy contribution are calculated as

$$\boldsymbol{f}_i^{M} = -\frac{\partial E}{\partial \boldsymbol{x}_i} \tag{24}$$

where the Helmholtz free energy of the network is [6, 7, 16, 17]

$$E = E_{i-p} + E_b + E_a + E_v \tag{25}$$

Consequently, it consists of the in-plane energy E_{i-p} (elastic + dissipative forces), the bending energy E_b defined as

$$E_b = \sum_i k_b \left(1 - \cos(\theta_i - \theta_0)\right) \tag{26}$$

the area conservation forces (global + local) E_a given by

$$E_a = k_a \frac{(A - A_0)^2}{2A_0} + \sum_i k_{ai} \frac{(A_i - A_{0i})^2}{2A_{0i}} \tag{27}$$

and the volume conservation forces E_v

$$E_v = k_v \frac{(V - V_0)^2}{2V_0} \tag{28}$$

where k_b is the bending constant, k_a, k_{ai} are the global and local area constraint constants and k_v is the volume constraint constant. The spontaneous angle between two adjacent triangles is denoted as θ and the instantaneous angle is

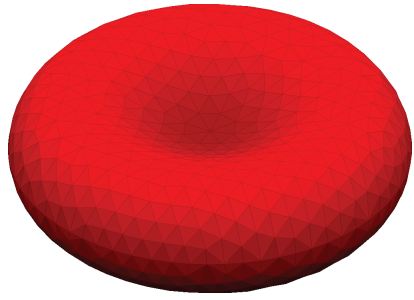

Figure 6. Spectrin network

θ_0. The total area and volume of red blood cells are A, V, respectively, and the spontaneous area and volumes are A_0, V_0. Finally, A_{0i} and A_i represent the local spontaneous and instantaneous areas, respectively.

4.5. Elastic immersed boundary model

Red blood cells consist of triangular meshes. Geometrical components of these meshes, such as edges, angles, surfaces and volume are utilised in order to simulate elastic properties of red blood cells. These include, inter alia, stretching and bending. The difference between the instantaneous and spontaneous shape of red blood cells is proportional to the magnitude of forces. Equation (23) describes the force exerted on a vertex. The elastic properties of red blood cells are modelled by $\boldsymbol{f}_i^M$ which consist of [5]

$$\boldsymbol{f}_i^M = \boldsymbol{f}_s + \boldsymbol{f}_b + \boldsymbol{f}_a + \boldsymbol{f}_A + \boldsymbol{f}_V \tag{29}$$

Similarly to other models, the individual mesh vertex of the red blood cell membrane moves according to equation (12).

Stretching forces express an inclination to preserve the spontaneous RBC shape and are given by the following formula

$$\boldsymbol{f}_s = k_s \kappa \frac{\Delta L}{L_0} \hat{\boldsymbol{n}} \tag{30}$$

where k_s is the stretching coefficient. The non-linearity of these forces is represented by

$$\kappa = \frac{(L/L_0)^{\frac{1}{2}} + (L/L_0)^{-\frac{5}{2}}}{L/L_0 + (L/L_0)^{-3}} \tag{31}$$

The spontaneous edge length is denoted here as L_0, whereas the instantaneous length by L, the difference between these two being ΔL. Finally, $\hat{\boldsymbol{n}}$ stands for the unit vector along the edge.

Bending forces are related to two adjacent triangles. They preserve the spontaneous angles between them. The force is expressed as

$$\boldsymbol{f}_b = k_b \frac{\Delta\theta}{\theta_0} \hat{\boldsymbol{n}} \tag{32}$$

This time $\hat{\boldsymbol{n}}$ represents the unit vector to a triangle. The bending coefficient is denoted as k_b, θ_0 and θ represent the spontaneous and instantaneous angles, respectively. Finally, $\Delta\theta$ is the deviation between them.

In order to preserve the spontaneous area of triangles, local area conservation forces have to be introduced

$$\boldsymbol{f}_a = k_a \frac{\Delta S_a}{S_{a0}} \hat{\boldsymbol{w}} \tag{33}$$

By $\hat{\boldsymbol{w}}$ one understands the unit vector from the centre of a triangle to the individual vertex. This means that there are three forces associated with the three vertices of a triangle. The local area coefficient is k_a, S_{a0} is the spontaneous area of a triangle and ΔS_a is the deviation from the spontaneous state. Similarly, global area conservation forces are given by

$$\boldsymbol{f}_A = k_A \frac{\Delta S}{S_0} \hat{\boldsymbol{w}} \tag{34}$$

Finally, volume conservation forces are expressed as

$$\boldsymbol{f}_V = k_V \frac{\Delta V}{V_0} S_a \hat{\boldsymbol{n}} \tag{35}$$

where k_V is the volume coefficient, S_a – the area of an individual triangle, V_0 – the spontaneous volume and ΔV – the deviation from it. $\hat{\boldsymbol{n}}$ stands for the unit normal vector to a triangle. Additionally, coupling of the red blood cell membranes with blood plasma is necessary, resulting in the fluid-structure interaction forces $\boldsymbol{f}_i^{FS}$. This can be achieved by means of the lattice Boltzmann method, which is described earlier.

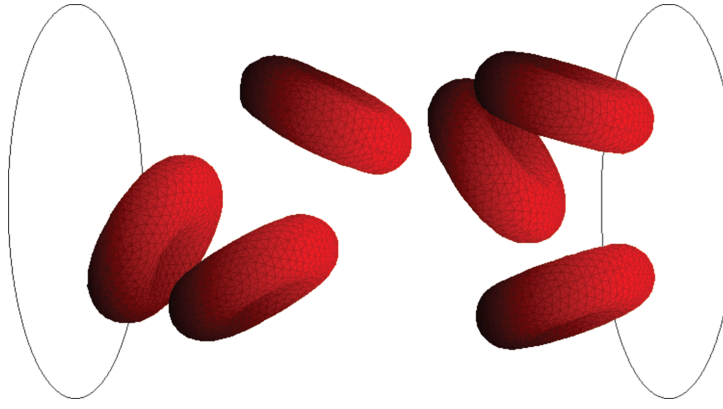

Figure 7. Simulation of several RBCs by means of the elastic immersed boundary model

Figure 7 displays example simulation results of several flexible red blood cells in the Hagen-Poiseuille flow. As previously, this can be classified as a semi-continuum model with a continuum fluid and discrete red blood cells.

5. Conclusions

Several approaches to blood flow modelling have been presented with particular attention paid to mesoscale semi-continuum models. The presented results can be also classified as passive transport of discrete and flexible red blood

cells in the Hagen-Poiseuille flow. Mesoscale models and explicit modelling of RBCs are required for capillaries when diameters are below 100 μm. The spring-damper model is the simplest and least accurate. What is more, it is difficult to control and maintain the shape of red blood cells. Furthermore, the spectrin network model is far more accurate and at the same time much more complicated and computer resource demanding. Finally, the elastic immersed boundary model appears to be a trade-off between accuracy and speed. This means that this approach is particularly suitable for real-time visualisation of the blood flow.

References

[1] MacMeccan R M, Clausen J R, Neitzel G P and Aidun C K 2008 *J. Fluid Mech.* **618** 13
[2] Zhang J, Johnson P C and Popel A S 2008 *J. Biomech* **41** (1) 47
[3] Ye T, Phan-Thien N, Khoo B C and Lim C T 2014 *Physics of Fluids* **26** 111902
[4] Moreno N, Vignal P, Lic J and Calo V M 2013 *Procedia Computer Science* **18** 2565
[5] Cimrak I, Gusenbauer M and Jancigova I 2014 *Computer Physics Communications* **185** 900
[6] Reasor Jr D A, Clausen J R and Aidun C K 2012 *Int. J. Numer. Meth. Fluids* **68** 767
[7] Discher D E, Boal D H and Boey S K 1998 *Biophysical Journal* **75** 1584
[8] Yilmaz F and Gundogdu M Y 2008 *Korea-Australia Rheology Journal* **20** (4) 197
[9] Astarita G and Marrucci G 1974 *Principles of non-Newtonian Fluid Mechanics*, McGraw-Hill
[10] Tesch K 2012 *Task Quarterly* **16** (3–4) 253
[11] Yamaguchi T, Ishikawa T, Tsubota K, Imai Y, Nakamura M and Fukui T 2006 *J. Biomechanical Science and Engineering* **1** (1) 29
[12] Atherton M A, Tesch K and Collins M W 2002 *Biorheology* **39** (3–4) 501
[13] Tesch K and Kaczorowska K 2016 *Engineering Optimization* **48** (3) 497
[14] Hoogerbrugge P J and Koelman J M V A 1992 *Europhys. Lett.* **19** 155
[15] He A and Luo L 1997 *Physical Review E* **55** (6), R6333
[16] Fedosov D A, Caswell B and Karniadakis G A 2009, 31st Annual International Conf. of the IEEE EMBS Minneapolis, Minnesota, USA
[17] Clausen J R, Reasor Jr D A and Aidun C A 2010 *Computer Physics Communications* **181** 1013